Title
SYNTHESIS OF HYDROCARBON FROM CO AND H? OVER SILICA-SUPPORTED RU: REACTION RATE MEASUREMENTS AND INFRARED SPECTRA OF ADSORBED SPECIES

Author
Ekerdt, John G.

Publication Date
1978-08-01

Submitted to Journal of Catalysis

LBL-8063
Preprint

SYNTHESIS OF HYDROCARBON FROM CO AND H_2 OVER SILICA-SUPPORTED RU: REACTION RATE MEASUREMENTS AND INFRARED SPECTRA OF ADSORBED SPECIES

John G. Ekerdt and Alexis T. Bell

August 1978

Prepared for the U.S. Department of Energy
under Contract W-7405-ENG-48

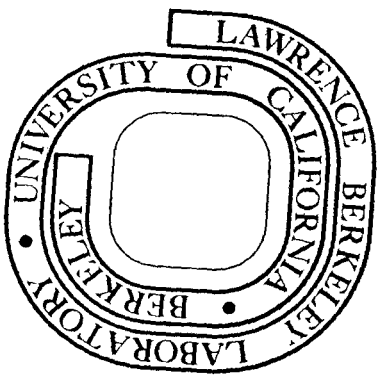

DISCLAIMER

LBL-8063

Synthesis of Hydrocarbon from CO and H_2 Over Silica-Supported Ru: Reaction Rate Measurements and Infrared Spectra of Adsorbed Species

by

John G. Ekerdt and Alexis T. Bell
Materials and Molecular Research Division
Lawrence Berkeley Laboratory

and

Department of Chemical Engineering
University of California, Berkeley, CA 94720

Abstract

The synthesis of hydrocarbons from CO and H_2 was studied on a silica-supported Ru catalyst and the species present on the catalyst surface were characterized by infrared spectroscopy. Initial rates of methane formation were correlated by the expression $N_{CH_4} = 7.4 \times 10^5 \exp(-24{,}000/RT) P_{H_2}^{1.5} / P_{CO}^{0.6}$. The synthesis of ethane, propylene, and propane, the principle products observed in addition to methane, was favored at high CO partial pressures, low H_2/CO ratios, and low temperatures. The primary feature observed in the infrared spectra was a band at 2030 cm^{-1}, associated with chemisorbed CO. Neither the position nor intensity of this band was affected by the CO partial pressure or the H_2/CO ratio. The CO band intensity did

decrease with increasing temperature due to a decrease in CO surface coverage. Bands were also observed at 2950, 2910, and 2845 cm^{-1} and were assigned to hydrocarbon structures surrounded by chemisorbed CO. These structures could be removed from the catalyst surface by hydrogenation, but do not appear to be intermediates in the synthesis of stable products. Reduction of the catalyst following steady state reaction revealed that the working catalyst maintains a reservoir of carbon several Ru monolayers in magnitude. A part of the carbon appears to be dissolved in the Ru but all of it readily reacts with H_2 to form methane, ethane, and propane. Carbon deposition mechanisms and the role of carbon in the synthesis of hydrocarbons are discussed.

INTRODUCTION

The characteristics of ruthenium catalysts for the synthesis of methane and higher molecular weight hydrocarbons from CO and H_2 have been discussed in a number of recent publications (1-11). Prime motivations for the interest in ruthenium have been its very high specific activity for methane synthesis and its high slectivity for the formation of straight-chained hydrocarbons. Concurrent with studies of overall catalyst performance efforts have been undertaken to define the elementary processes involved in the conversion of CO and H_2 to hydrocarbons. In this context, attention has focused on two principle questions. The first is whether synthesis is initiated by the direct hydrogenation of adsorbed CO to form an oxygenated intermediate or by the dissociation of adsorbed CO to form carbon, which is subsequently hydrogenated. The second major question is whether propagation of carbon chains occurs by CO insertion into adsorbed alkyl-type intermediates or by polymerization of CH_x fragments. Arguments for both sides of these questions can be found in the literature.

Support for the direct hydrogenation of chemisorbed CO has come mainly from the interpretation of kinetic data. Vannice (6) and Ollis and Vannice (8) have proposed that methanation over Ru and other group VIII metals is initiated by the reversible hydrogenation of chemisorbed CO to form an enol intermediate. The rate determining step is taken to be the further hydrogenation of the initial intermediate. Based upon this hypothesis, rate expressions were developed which

could be made consistent with those observed experimentally. Direct hydrogenation of chemisorbed CO to form an oxygenated intermediate has also been proposed as the first stage in Fischer-Tropsch synthesis by Dautzenberg et al. (9). Chain growth is envisioned to occur by repeated CO insertion into the primary intermediate followed by hydrogenation. Using this mechanism the authors developed a kinetic model to correlate product distribution data obtained from transient response experiments.

Experimental evidence supporting the idea that CO dissociation to form carbon is an essential initial step in the synthesis of methane has recently been presented by Rabo et al. (12). In studies with silica-supported Ru these authors observed that at 300°C passage of CO pulses over the catalyst led to the formation of CO_2 and the deposition of carbon on the catalyst surface. The carbon thus deposited could be hydrogenated to produce methane at room temperature. No methane was observed under similar conditions when only chemisorbed CO was present on the catalyst. Similar results have also been obtained by McCarty et al. (13) and Low and Bell (14). Further support for CO dissociation as an important step has come from the work of Dalla Betta and Shelef (4). The absence of an H_2/D_2 kinetic isotope effect on the rate of methane formation was taken as evidence that CO dissociation might be a rate determining step.

Several studies have been undertaken to observe Fischer-Tropsch intermediates by infrared spectroscopy. Dalla Betta and Shelef (3) and King (15) have observed that the

primary species present on an alumina-supported Ru catalyst is chemisorbed CO. Hydrocarbon and formate species were also evident but isotopic substitution experiments (3) led to the conclusion that these structures were inactive reaction products adsorbed on the alumina support. Infrared investigations have also been carried out on silica-supported Ru catalysts by Ekerdt and Bell (16) and King (15). Here again adsorbed CO was observed as the primary adspecies. Hydrocarbon species were also detected but there was no evidence of the formate structure seen on alumina.

The present studies were undertaken to further investigate the mechanism and kinetics of hydrocarbon synthesis over Ru. An important objective of this effort was to determine the role of chemisorbed CO in both the initiation and propagation of hydrocarbon synthesis. For these studies in situ infrared spectroscopy was combined with measurements of reaction rates both under steady state and transient conditions.

EXPERIMENTAL METHODS

Apparatus

The reactor used in this work is shown in Fig. 1. It was designed to fit within the sample compartment of a Perkin Elmer 467 infrared spectrometer so that infrared spectra of species adsorbed on the catalyst surface could be recorded under reaction conditions. The rectangular inner chamber of the reactor is made of stainless steel and is aluminum coated on the inner surfaces to reduce the catalytic activity of the walls. The infrared beam passages through

this chamber are covered by ZnSe windows sealed to knife-edge flanges by Vac-Seal. Strip heaters placed on the top and bottom of the chamber allow it to be heated to 300°C, an upper limit set by the use of ZnSe windows. The outer chamber is also made of stainless steel but the beam passages through this chamber are covered by KBr windows. To minimize heat losses the space between the two chambers is evacuated.

A catalyst wafer, 25 mm in diameter and weighing 180 mg, is supported on the sample side of the inner chamber of the reactor. A second wafer, made of the catalyst support alone, is supported on the reference side of the inner chamber. The wafer temperatures are monitored by stainless steel sheathed thermocouples positioned adjacent to each wafer. By using two wafers, the superposition of the catalyst support spectrum on the recorded spectrum is minimized. Furthermore, due to the identical path lengths through the sample and reference sides of the inner chamber the gas phase spectrum is also suppressed.

The reactor is connected to a gas flow system. To insure a nearly uniform gas composition within the reactor, gas is recirculated from the inlet to the outlet of the reactor by a 40 ℓ/min stainless steel bellows pump. Reactants are introduced into the recirculating gases and a comparable flow of products is removed continually. During the measurement of reaction kinetics the recycle ratio is maintained at 200 to 1 to assure differential conversion per pass through the reactor. To avoid flowing hot reactants and products through the pump, the gas leaving the reactor is

cooled in a length of aluminum tubing prior to entering the pump and heated in a second length of aluminum tubing upon leaving the pump and returning to the reactor. The effluent from the gas recirculation loop is passed through a dry ice trap to remove water and then analyzed by gas chromatography. A 124 cm column packed with Porapak Q is used to separate all of the reaction products.

Materials

A 5% Ru/SiO_2 catalyst was prepared by impregnating Cab-O-Sil HS-5 with a solution of $RuCl_3 \cdot 3H_2O$. The slurry was freeze-dried and then reduced for 2 hrs. in flowing hydrogen 400°C. The surface area of the reduced catalyst was determined by H_2 chemisorption. Prior to measuring the H_2 uptake the catalyst was reduced in H_2 at 400°C for 2 hrs. and then evacuated at 400°C for 2 hrs. Chemisorption was then carried out at 100°C in 400 torr of H_2 (17). The equilibrium uptake was determined to be 22 μmoles of H_2 per gram of catalyst. Rates reported here as turnover numbers were determined using H_2 uptake as a measure of Ru surface area.

The gases H_2 (99.999%), D_2 (99.7%), and He (99.998%) were used without further purification. Carbon monoxide (99.8%) was purified by passage through a trap of dry ice prior to entering the reactor.

RESULTS

Kinetic Measurements

Preceeding each measurement of reaction kinetics the catalyst was reduced overnight in flowing H_2 at the intended

reaction temperature. Following the introduction of the reaction mixture the gas composition was analyzed as a function of time. Figure 2 illustrates an example of the data. The points show that the rate of methane formation, relative to the initial rate measured at 10 min, declines as a function of time, indicating a loss in catalyst activity. The rate of deactivation is seen to increase as the ratio of H_2 to CO over the catalyst is decreased. For a fixed H_2/CO ratio the deactivation rate is also observed to increase with CO partial pressure as shown in Fig. 3. The catalyst deactivation is reversible, however, and the original activity can be restored by heating the catalyst overnight in flowing H_2 at temperatures between 190 and 275°C.

To minimize the influence of deactivation on the measured kinetics, only the initial rates, measured at 10 min, were used. Data were taken at CO partial pressures between 16 and 200 torr, H_2/CO ratios between 1 and 20, and temperatures between 191 and 275°C. The CO conversions observed ranged from 0.1% for the lowest reaction rates to 40% for the highest rates. As exemplified by the data shown in the legends of Figs. 2 and 3, the rate of methane formation was observed to increase with H_2/CO ratio at a constant CO partial pressure and to increase with CO partial pressure at a constant H_2/CO ratio.

The dependence of the rate of methane formation on the partial pressures of H_2 and CO was determined by a nonlinear least square fit of the accumulated rate data to the following empirical expression

$$N_{CH_4} = Ae^{-E/RT} P_{H_2}^{X} P_{CO}^{Y} \qquad (1)$$

where N_{CH_4} is the rate of methane production per surface Ru site, where A is the pre-exponential factor, E the apparent activation energy, and X and Y are exponents on the partial pressures of H_2 and CO respectively. The quality of the fit between the data and eqn. 1 is shown in Fig. 4. Over three orders of magnitude in N_{CH_4}, the average absolute relative deviation between the calculated and observed turnover numbers is $\pm$15%.

In addition to methane, the products were found to contain ethane, propylene and propane. Ethylene, when detected, was present only in trace quantities and its concentration could not be determined accurately. The yields of higher molecular weight products were independent of catalyst deactivation, indicating that overall activity as well as methanation activity decays with time. The dependence of product distribution on reaction conditions is shown in Figs. 5 through 7. It is apparent that the formation of high relative yields of C_2 and C_3 products is favored as the temperature and the H_2/CO ratio decrease and as the partial pressure of CO increases. A particularly interesting product composition was obtained when the temperature was set to 191°K, the CO partial pressure to 195 torr, and the H_2/CO ratio to 2. Under these conditions only propylene was observed in addition to methane and the propylene to methane ratio was essentially one to one.

The only nonhydrocarbon product observed in significant concentrations was water. Carbon dioxide was detected but its concentration was negligible compared to that of water. These results indicate that the reaction products are far from equilibrium with respect to the water gas shift reaction.

In Situ Infrared Spectroscopy

Fig. 8 shows typical infrared spectra recorded under reaction conditions at 191, 225, and 275°C. At all three temperatures the most prominant feature is a strong band at 2030 cm^{-1}, characteristic of CO linearly adsorbed on a fully reduced silica-supported Ru catalyst (18,19). The position of the CO band remained constant to within ± 5 cm^{-1} for all of the reaction conditions used in this work and did not change as the catalyst deactivated. The dependence of the CO band absorbance on reaction conditions is shown in Fig. 9. The data points show that at a fixed temperature the absorbance is essentially independent of either the CO partial pressure or the H_2/CO ratio. Whatever variations are observed are well within the scatter of the data. While not noted in Fig. 9, it was found that the band intensity was also independent of the extent of catalyst deactivation. To further test whether the presence of H_2 affects the intensity of the CO band, the catalyst was contacted with CO/He mixtures in which the CO partial pressures were similar to those used under reaction conditions. The resulting spectra showed a CO band centered at 2030 cm^{-1}, identical in shape to that shown in Fig. 8. At each temperature, the CO band absorbance was essentially the same as that given by the horizontal lines

shown in Fig. 9. The only variable found to influence the CO band intensity was temperature. Both in the absence and presence of H_2 the band intensity was observed to decrease with increasing temperature.

Spectrum d in Fig. 6 shows three bands at 2950, 2910 and 2845 cm^{-1} in addition to the CO band at 2030 cm^{-1}. These new features are observed only at 191°C and only when the CO partial pressure is above 180 torr and the H_2/CO ratio is below 2. The bands increase in intensity very slowly and become prominant only after 20 min. Based upon the positions of the bands, the weak shoulder appearing at 2950 cm^{-1} can be assigned to C-H stretching vibrations in methyl groups while the two more intense peaks at 2910 and 2845 cm^{-1} can be assigned to symmetric and asymmetric C-H vibrations in methylene groups (20).

To determine whether the observed C-H stretching frequencies might be due to the adsorption of hydrocarbon products on either the Ru or the support a gas mixture containing CO, CH_4, C_2H_4, C_2H_6, C_3H_6, C_3H_8, and CO_2 was passed over the catalyst at 191°C. No absorbtion bands were observed. This indicates that the hydrocarbon adspecies giving rise to the bands in the vicinity of 2900 cm^{-1} are not reaction products adsorbed from the gas phase, but rather adspecies formed during the course of the reaction.

A number of experiments were performed to determine the stability and reactivity of the adsorbed hydrocarbon species and their possible role in the formation of reaction products. In the first experiment a mixture of CO and H_2

was fed to the reactor, maintained at 191°C, for 1 hr. The feed was then switched to a CO and D_2 mixture for 1 hr and then finally back to the original feed. It was observed that the bands at 2950, 2910 and 2845 cm^{-1} remained unchanged upon substitution of D_2 for H_2 but that a new set of bands were formed at 2210, 2180 and 2090 cm^{-1}, corresponding to the fully deuterated forms of the hydrocarbon adspecies. Upon return to the feed containing H_2, the bands associated with the deuterated structures stopped growing and the bands corresponding to the hydrogen containing structures resumed their growth.

In the second experiment, a run was first carried out at 191°C. At the end of the run, the flow of H_2 was stopped and the flow of CO and He continued until H_2 had been eluted from the reactor. The CO flow was then terminated and CO was eluted from the reactor by a flow of He. Spectra of the surface taken after the elution of H_2 and CO are shown in Fig. 10. Spectrum b is identical to that recorded under reaction conditions. Spectrum c taken after the elution of CO, shows that the CO band has shifted to 1940 cm^{-1} and diminished somewhat in intensity. The shift in the CO band frequency from 2030 cm^{-1} to 1940 cm^{-1} suggests that a fraction of the CO monolayer has desorbed and that the remaining adsorbed CO is strongly bonded, possibly in a bridged fashion (21). It is important to note, however, that the adspecies responsible for the hydrocarbon bands are stable even in the absence of gas phase H_2 and CO.

Following the elution of CO in the experiment just described, a flow of H_2 in He was introduced into the reactor. Spectra taken subsequently show that the bands associated with the hydrocarbon species and the CO band are rapidly attenuated and within 4 min are completely removed from the spectrum. These observations show that the hydrocarbon species are stable in the presence of adsorbed CO but are rapidly hydrogenated once CO is removed from the catalyst surface.

Reduction of Carbonaceous Residues

Following each steady-state experiment the flow of CO to the reactor was stopped but the flow of H_2 and He was continued. The purpose of this procedure was to flush the reactor of CO and to remove any carbonaceous residues from the catalyst by reaction with H_2. Reactor effluent compositions and infrared spectra taken during this period provided important information with regard to the identity and reactivity of the species present on the catalyst surface at the end of a run.

Figures 11 and 13 show the relative absorbance of the CO band, appearing at 2030 cm^{-1}, as a function of the time since termination of the CO flow. The curves for all four runs are qualitatively similar. Initially the relative absorbance remains constant at unity and then at a well defined moment falls rapidly to zero. Similar patterns were also observed at 225 and 275°C. As the temperature is increased the time at which the CO band disappears becomes shorter.

To interpret the curves of CO absorbance versus time it is necessary to know the time dependence of the CO partial pressure in the gas phase. Unfortunately, over the time span shown in Figs. 11 and 13 only one gas sample could be analyzed. The CO partial pressures determined from these analyses divided by the steady state CO partial pressures are indicated by the isolated data points. Since there is so little composition data, an upper bound on the CO partial pressure is shown as well. The straight lines appearing in Figs. 11 and 13 are given by

$$P_{CO}(t)/P_{CO}(0) = e^{-t/\tau} \qquad (2)$$

which represents the time dependence of a nonreacting component eluted from a well-stirred vessel (22). The parameter τ in eqn. 2 represents the reactor space time (typically 2.6 min.). The location of the measured values of $P_{CO}(t)/P_{CO}(0)$ show that the CO partial pressure falls off more rapidly than predicted by eqn. 2, thereby indicating that a fraction of the CO reacts as it is eluted.

The curves of relative CO absorbance can now be understood by recognizing that as long as the CO partial pressure is sufficiently high, the Ru surface remains essentially saturated with CO and the relative absorbance is unity. Once the CO partial pressure becomes significantly less than a torr the readsorption rate can no longer keep up with the rate of CO removal from the surface and the relative absorbance falls. Consistent with this picture we observe that the time at which the decay in absorbance

begins depends upon the CO partial pressure used at steady state but is independent of the steady state H_2/CO ratio. The slight displacement in curves for the two runs shown in Fig. 13 is totally due to the differences in the flow rates of the H_2/He streams used in these runs.

The decay in CO absorbance which occurs at low CO pressures could either be due to desorption or reaction with H_2. The first of these possibilities can be excluded based upon experiments in which He alone was used to elute the CO. During these experiments the CO absorbance remained at near saturation levels even though the CO partial pressure was reduced to the order of 10^{-3} torr. On the other hand, when H_2 was present in the eluting gas, the chemisorbed CO could be removed from the surface at CO partial pressures of the order of one torr.

Figures 12 and 14 show the relative rates of methane and ethane-production during reduction. For each run the curves for both components pass through a maximum at about the same time that the CO absorbance goes to zero (as indicated by the vertical arrows). Beyond the maximum, the relative rate of methane formation falls off gradually but the relative rate of ethane formation declines rapidly to zero. While the curves for methane shown in Figs. 12 and 14 terminate at 35 min., data were usually collected for 125 min. The magnitude of the maxima in the methane and ethane curves and the level of the slowly decaying portion of the methane curve increase as either the steady state partial pressure of CO or the H_2/CO ratio is decreased. It should be noted,

however, that the absolute rate of methane production measured at 35 min increases with both CO partial pressure and H_2/CO ratio.

The observation of hydrocarbon formation long after CO has been eluted from the gas phase and removed from the catalyst surface is enhanced by increasing the steady state partial pressure of CO and decreasing the ratio of H_2/CO. Figure 15 illustrates the rates at which methane and ethane are formed during reduction following a run at 191°C in which the feed partial pressure of CO was 195 torr and the H_2/CO ratio was 2.0. In contrast to the results shown in Figs. 12 and 14, ethane formation continues for a long time beyond the point at which CO is present either in the gas phase or on the surface of the catalyst. While not shown in Fig. 15, small amounts of propane were also observed during the reduction period. It is interesting to note that when the catalyst was operated at steady-state neither ethane nor propane was observed and only methane and propylene were detected.

The shape of the curves appearing in Figs. 12, 14 and 15 can be interpreted in the following fashion. Upon cessation of the CO flow, the H_2 partial pressure in the H_2/He feed stream is set to about 290 torr. This causes the CO partial pressure to steadily decline while the H_2 partial pressure changes from the value held during steady state to that in the H_2/He feed stream. The net result is a very rapid increase in the H_2/CO ratio of the gas within the

reactor. In response to this change the rate of hydrocarbon production increases. For the case of methane the response to the decrease in CO partial pressure is predicted by eqn. 1. Consistent with the proposed interpretation we observe that the extent to which the steady-state rate of hydrocarbon formation is surpassed depends upon the CO partial pressure and the H_2/CO ratio maintained during the steady-state period. The lower the CO partial pressure or the H_2/CO ratio, the greater is the net rise over the steady-state reaction rate.

The appearance of a maximum in the curves of relative rate of hydrocarbon formation closely coincides with the complete elution of CO from the reactor gas space and the elimination of CO from the catalyst surface. This feature suggests that at very low CO partial pressures the rate of hydrocarbon formation becomes positive order in CO, in response to CO adsorption becoming a rate limiting step.

The continued formation of hydrocarbon products long after CO has been excluded from the reactor and the catalyst surface, is the most interesting characteristic of the data shown in Figs. 12, 14 and 15. In addition, it is seen that the rate of methane formation is comparable to the steady-state rates for extended periods of time. These observations suggest that the hydrocarbon products observed are formed by hydrogenation of a carbonaceous species on the catalyst surface and that these same species may be responsible for product formation under steady-state reaction conditions.

To further confirm the idea that hydrogenation of carbonaceous residues present on the catalyst surface could produce methane and ethane, the following experiment was carried out. Upon completion of a steady-state run at 191°C, first H_2 and then CO was eluted from the reactor. A flow of H_2 in He was then introduced. Infrared spectra taken after the addition of H_2 showed that within 4 min all of the adsorbed CO had been removed from the surface. The subsequent rates of methane and ethane formation were observed as functions of time and are shown by the triangular data points in Fig. 15. It is apparent that the initial rate of methane production is nearly a hundred-fold higher than that observed at steady-state and that even after 125 min of reaction the rate is a factor of two greater than the steady-state rate. While no ethane was produced during the steady-state period it is seen that a significant amount of ethane appears during the hydrogenation of the carbonaceous residue. Adsorption of the product gases, formed during the first 5 min of reduction, on activated carbon and subsequent mass spectrometric analyses of the desorbed gases revealed that small amounts of propane were also produced during the early stages of reduction.

The total amounts of carbon removed from the catalyst as methane and ethane are shown in Table 2. These figures were obtained by integrating the production of each component. Integration was started at a point 2.3 space times (approximately 6 min) beyond the time at which the CO band disappeared from the spectrum and was terminated at the

time when the rate of product formation became negligibly small. The total number of moles of carbon removed from the catalyst is in most instances greater than the number of Ru surface sites (7.9×10^{-6} moles) and is clearly dependent upon the reaction conditions under which the carbon is deposited. The table shows that for a constant inlet partial pressure of CO and H_2/CO ratio the amount of carbon deposited increases with the reaction temperature. In addition, at a constant temperature the carbon deposited increases with both the inlet partial pressure of CO and the H_2/CO ratio. It is also evident that the amount of carbon deposited is independent of the duration of a steady-state run carried out at 191°C.

To determine whether the amount of carbon deposited under reaction conditions was different from that deposited upon exposure of the catalyst to CO alone, a run was carried out in which the catalyst was maintained at 191°C in a CO/He flow for 70 min. Following this exposure, the flow of CO was discontinued and a stream containing H_2 in He was introduced into the reactor. Table 2 shows that the amount of carbon removed as methane is considerably smaller than that observed after a reaction run.

DISCUSSION

The kinetics of methane formation reported here are correlated by eqn. 1, using the values of X, Y, A, and E given in Table 1. Similar rate expressions have been reported by Dalla Betta et al. (1) and Vannice (6,7) and

the rate parameters found in those studies are also shown in Table 1. There is general agreement among all three investigations concerning the order with respect to H_2 partial pressure, but the order with respect to CO shows a wider spread. The results of this investigation and that of Vannice indicate a nearly inverse half order dependence while that of Dalla Betta et al. favors a roughly inverse first order CO dependence. The agreement with regard to the apparent activation energy is very good, all three groups reporting a value of about 24 Kcal/mole. There is greater disagreement, however, concerning the magnitude of the pre-exponential, A. Differences in this parameter are very hard to reconcile since the specific activity of Ru catalysts can depend upon the dispersion (l_0) and the accuracy with which the Ru surface area was measured (17).

The infrared spectra taken under reaction conditions show that at a fixed temperature neither the CO partial pressure nor the H_2/CO ratio affects the frequency or intensity of the CO band appearing at 2030 cm^{-1}. In addition the band position and intensity are identical to those observed when CO is adsorbed in the absence of H_2. These observations differ from those of Dalla Betta and Shelef (3). In their investigation with an alumina-supported Ru catalyst it was found that the CO band which appeared at 2043 cm^{-1} in the absence of H_2 shifted to 1996 cm^{-1} when H_2 was present in 3 to 1 ratio with CO. The occurence of a frequency shift was used to argue that adsorbed H_2 contributed to a weakening

of the C-O bond. The absence of a shift in the CO band position when CO and H_2 are coadsorbed on a silica-supported Ru catalyst might be regarded as an indication of the differences between alumina and silica-supported Ru. However, the nature of these differences cannot be explained at this time.

The results presented in Fig. 9 show that the intensity of the CO band decreases as the temperature increases but that the band intensity is essentially independent of CO partial pressure and H_2/CO ratio at each temperature. These observations can be interpreted by comparison of the data in Fig. 9 with CO adsorption isotherms. Figure 16 illustrates a series of isotherms measured gravimetrically on a silica-supported Ru catalyst very similar to that used in the present studies (24). For a fixed CO pressure the coverage by adsorbed CO is seen to be a strong function of temperature. By contrast, CO coverage changes more slowly as the CO pressure is increased at a fixed temperature. The decrease in CO absorbance with increasing temperature, seen in Fig. 9, can, thus, be ascribed to a decrease in the coverage by adsorbed CO. The absence of a dependence on CO band intensity on H_2/CO for a fixed CO partial pressure suggests that H_2 adsorption does not interfere with CO adsorption and that the reaction of chemisorbed CO is slow by comparison with desorption. As a result, the presence of H_2 does not influence the chemisorption equilibrium for CO. The failure to observe an increase in CO band intensity with CO partial pressure is

surprising in view of the adsorption data shown in Fig. 16. A possible explanation may lie in the decision to use maximum absorbance as a measure of CO coverage rather than integrated band absorbance.

The hydrocarbon bands in the vicinity of 2900 cm^{-1} which have been observed in this work are very similar to those seen by King (14) on silica-supported Ru and by Dalla Betta and Shelef (3) and King (15) on alumina-supported Ru. In view of the stability and reactivity patterns exhibited by the species responsible for the observed bands it seems reasonable to conclude that these species are present on the Ru rather than on the support. While it is not possible to establish the structure of the hydrocarbon species, it is of interest to note that Eady et al. (23) have recently reported the formation of various Ru clusters containing carbene, ethylidene, ethylidyne, and ethylenic structures. These products were formed by reaction of $Ru_3(CO)_{12}$ with $Na[BH_4]$. It is conceivable that the species formed in the present work are similar to those observed by Eady et al. The occurrence of hydrocarbon species surrounded by adsorbed CO might explain the stability of these species to hydrogenation under reaction conditions and the ease with which they can be hydrogenated once the adsorbed CO is removed from the Ru surface.

The results presented in Table 2 show that under reaction conditions the catalyst maintains a carbon reservoir in excess of a monolayer. Furthermore, as seen in Figs. 12, 14 and 15 this carbon is very reactive and in the absence of CO on the surface can be hydrogenated to produce methane, ethane, and propane. The rate of methane production is equivalent to or greatly in excess of that measured under steady state conditions. These observations lead to the consideration of carbon as an important intermediate not only for methane formation but also for the synthesis of higher molecular weight products. In this context it is important to discuss the origin of the carbon deposit, the influence of reaction conditions on the magnitude of the deposit, and the mechanisms by which carbon is converted to methane and other hydrocarbon products.

Rabo et al. (12), McCarty et al. (13), and Low and Bell (14) have observed that carbon deposition can occur on the surface of Ru during CO adsorption at temperatures above about 150°C (14). This process is accompanied by the formation of CO_2 and is believed to occur by the following steps (12):

1. $CO + S \rightleftarrows CO_s$
2. $CO_s + S \rightleftarrows C_s + O_s$
3. $O_s + CO \rightarrow CO_2$

McCarty et al. (13) have estimated that the equilibrium constant for reaction 2 is unfavorable due to the high

endothermicity of the reaction (~21 Kcal/mole) and that, as a result, reaction 3 plays an important role in shifting the equilibrium towards the formation of carbon. When H_2 is present in addition to CO, the removal of surface oxygen is further enhanced by reaction 4

$$4.\quad O_s + H_2 \rightarrow H_2O$$

Both reactions 3 and 4 have been observed experimentally to proceed preferentially via Rideal-Eley type processes over Pt when CO or H_2 is present at moderate partial pressures [e.g. (25-31)]. While similar observations have not been made for Ru, we have assumed that oxygen removal occurs by a Rideal-Eley process for this catalyst as well. BEBO estimates of the activation energies for reactions 3 and 4 occurring over Ru give 0 and 17 Kcal/mole respectively (32,33). As a result, it is anticipated that for identical fluxes of reducing agent reaction 4 will be much more rapid than reaction 3 in effecting the removal of adsorbed oxygen atoms. Supporting this expectation is the observation that H_2O rather than CO_2 is observed as the major oxygen containing product under all synthesis conditions studied in this work. It is also seen in Table 2 that the amount of carbon deposited on the catalyst is significantly greater when CO and H_2 are present together than when CO is present alone.

The observation of greater than monolayer accumulations of carbon on the catalyst suggest that a part of the carbon

may dissolve into the bulk of the Ru. This idea is further supported by the observation that the intensity of the CO band associated with chemisorbed is not influenced by either the CO partial pressure of the H_2/CO ratio, while the amount of carbon present on the catalyst does depend upon these variables is shown in Table 2. Since Ru does not form stable carbides the dissolution of carbon in Ru crystallites could provide a rational interpretation for the observation.

A plausible mechanism for the hydrogenation of surface carbon to form methane is shown below. This reaction sequence

5. $H_2 + 2S \rightleftarrows 2H_s$

6. $C_s + H_s \rightleftarrows CH_s + S$

7. $CH_s + H_s \rightleftarrows CH_{2s} + S$

8. $CH_{2s} + H_s \rightleftarrows CH_{3s} + S$

9. $CH_{3s} + H_s \rightleftarrows CH_4 + S$

is nearly identical to that proposed by Wagner (34) to explain the formation of methane from carbon dissolved in γ-iron. If it is assumed that reaction 9 is rate limiting for the synthesis of methane; that reactions 1, 2 and 5 through 8 are at equilibrium; and that the catalyst surface is nearly saturated with chemisorbed CO, then the following expression is obtained for the rate of methane formation:

$$N_{CH_4} = k \frac{P_{H_2}^{1.5}}{P_{CO}} \qquad (3)$$

$$k = \frac{K_5}{K_1} (k_4 k_9 K_2 K_6 K_7 K_8)^{1/2} \qquad (4)$$

where k_i is the rate coefficient and K_i the equilibrium constant for the ith elementary reaction. Equation 3 has the same form as eqn. 1 and the exponent on the hydrogen partial pressure is nearly identical to that found experimentally. The inverse first order dependence on CO partial pressure given by eqn. 3 is greater, however, than the nearly inverse square root dependence observed experimentally. Selection of other rate limiting steps within the proposed sequence not only fails to reduce the dependence on CO partial pressure but also causes the hydrogen partial pressure dependence to deviate from that observed experimentally.

A rate expression more representative of the experimental results can be obtained if it is postulated that the rate limiting step is reaction 8' shown below.

$$8' \qquad CH_{2s} + H_2 \rightleftarrows CH_4 + S$$

Maintaining all of the previous assumptions, but substituting reaction 8' for reactions 8 and 9, the rate expression derived for methane formation becomes

$$N_{CH_4} = k' \frac{P_{H_2}^{1.5}}{P_{CO}^{0.5}} \qquad (5)$$

$$k' = (k_8, k_4 K_5 K_6 K_7 / K_1)^{1/2} \qquad (6)$$

While eqn. 5 is in closer agreement with the observed rate expression than eqn. 3, there has been no experimental evidence to suggest that reaction 8' proceeds as written.

The processes by which two- and three-carbon hydrocarbons are formed are not revealed by these studies, but it has been established that these products can be formed in the absence of adsorbed CO. One possibility is that adsorbed carbene groups, formed via reaction 7, polymerize and react according to the following scheme:

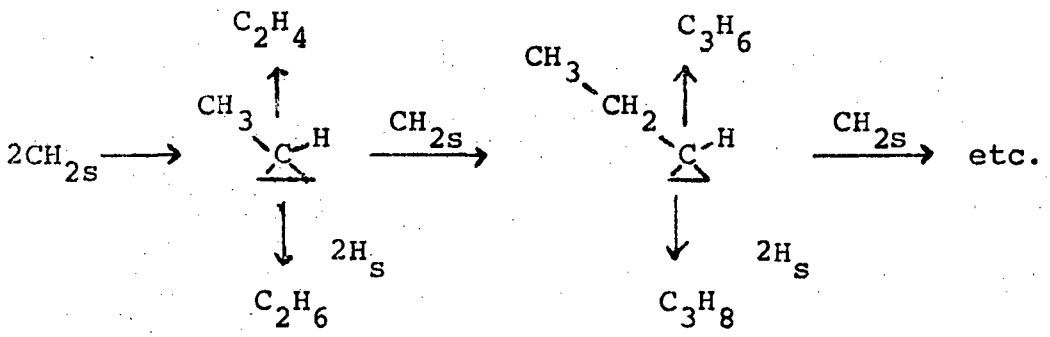

Carbenes have been observed as ligands in OS and Ru cluster complexes (23,35) and in a mononuclear Fe complex (36) and an ethylidene structure has recently been reported on the surface of Pt (37). Thus, it is not unreasonable to postulate these species as surface intermediates. Furthermore, given the known reactivity of gas phase carbenes and their metalorganic analogs it would appear likely that the chain propagation sequence proposed is possible.

The formation of olefins could occur by intramolecular hydrogen transfer within the appropriate carbene intermediate, followed by desorption. Some evidence supporting such a process can be derived from the reported chemistry of alkyl carbenes prepared from organometallic precursors (38). The

observed preferential formation of propylene over ethylene could possibly result from the greater ease with which a hydrogen atom is transferred from the methylene group of propylidene compared to the transfer of hydrogen from the methyl group of ethylidene. As an alternative one might propose that gas phase ethylene very rapidly reacts with surface carbene groups to form propylene, in analogy to known gas phase chemistry (38).

Finally, we note that the proposed propagation scheme can be used to predict a Schulz-Flory-type distribution of product molecular weights (39). To obtain such a distribution it is only necessary to postulate that steady state concentrations exist for H_s and CH_{2s}, and that the rate coefficients associated with propagation, desorption to form olefins, and hydrogenation to form alkanes are independent of carbon number. Thus, for example, the experimental results on product distribution recently reported by Dautzenberg et al. (9) could be interpreted by the mechanism proposed here.

ACKNOWLEDGMENT

The authors wish to acknowledge the many productive discussions of these results with Dr. H. Wise of SRI-International. This work was supported by the Division of Chemical Sciences, Office of Basic Energy Sciences, U.S. Department of Energy.

REFERENCES

1. Dalla Betta, R. A., Piken, A. G., and Shelef, M., J. Catal. 35, 54 (1974).
2. Dalla Betta, R. A., Piken, A. G., and Shelef, M., J. Catal. 40, 173 (1975).
3. Dalla Betta, R. A. and Shelef, M., J. Catal. 48, 111 (1977).
4. Dalla Betta, R. A. and Shelef, M., J. Catal. 49, 383 (1977).
5. Vannice, M. A., J. Catal. 37, 449 (1975).
6. Vannice, M. A., J. Catal. 37, 462 (1975).
7. Vannice, M. A., J. Catal. 50, 228 (1977).
8. Ollis, D. F. and Vannice, M. A., J. Catal. 37, 449 (1975).
9. Dautzenberg, F. M., Heller, J. N., Van Santen, R. A., and Verbeek, H., J. Catal. 50, 8(1977).
10. King, D. L., J. Catal. 51, 386 (1978).
11. Everson, R. C., Woodburn, E. T., and Kirk, A. R. M., J. Catal. 53, 186 (1978).
12. Rabo, J. A., Risch, and Poutsma, J. L., J. Catal. 53, 295 (1978).
13. McCarty, J., Wentrcek, P. and Wise, H., SRI-International, Menlo Park, CA, personal communication.
14. Low, G. G. and Bell, A. T., to be submitted to J. Catal.
15. King, D. L., Preprints, A. C. S. Div. of Petrol. Chem., 23(2), 482 (1978).
16. Ekerdt, J. G. and Bell, A. T., Preprints, A. C. S. Div. Petrol. Chem. 23(2), 475 (1978).
17. Taylor, K., J. Catal. 38, 299 (1975).
18. Brown, M. F. and Gonzalez, R. D., J. Phys. Chem. 80, 1731 (1976).

19. Davydov, A. A. and Bell, A. T., J. Catal. 49, 332 (1977).

20. Bellamy, L. J., "The Infrared Spectra of Complex Molecules" 3rd ed., John Wiley & Sons, New York, 1975.

21. Guerra, C. R., and Schulman, J. H., Surface Sci. 7, 229 (1967).

22. Levenspiel, O., "Chemical Reaction Engineering", 2nd ed., John Wiley & Sons, New York, 1972.

23. Eady, C. R., Johnson, B. F. G, and Lewis, J., J. C. S. Dalton, 477 (1977).

24. Bollinger, W. A., "Gravimetric Adsorption Study of Hydrogen and Carbon Monoxide on a Supported Ruthenium Catalyst", M. S. thesis, Department of Chemical Engineering, University of California, Berkeley, CA, 1976.

25. Bonzel, H. P., and Ku, J., J. Vac. Sci. & Tech. 9, 663 (1972).

26. Joebstl, J. A., J. Vac. Sci. & Tech. 12, 347 (1975).

27. Ducros, R., and Merrill, R. P., Surf. Sci. 55, 227 (1976).

28. Palmer, R. C., and Smith, J. N., J. Chem. Phys. 60, 1453 (1974).

29. Smith, J. N., and Palmer, R. L., J. Chem. Phys. 56, 13 (1972).

30. Bernasek, S. L., and Somorjai, G. A., J. Chem. Phys. 62, 3149 (1975).

31. Monroe, D. R., "The Structure and Chemistry of Oxygen Adsorbed on Pt(111) and its Reaction with Reducing Gases", Ph.D. thesis, Department of Chemical Engineering, University of California, Berkeley, CA, 1977.

32. Weinberg, W. H., and Merrill R. P., J. Catal. 40, 268 (1975).

33. Miyazaki, E., and Yasumori, I., Surf. Sci. 55, 747 (1976).

34. Wagner, C., Adv. Catal. 21, 323 (1970).

35. Deeming, A. J., and Underhill, M., J. C. S. Dalton, 1415 (1974).

36. Jolly, P. W., and Petit, R., J. A. C. S. 88, 5044 (1966).

37. Ibach, H., Hopster, H., and Sexton, B., Appl. Surf. Sci. 1, 1 (1977).

38. Krimse, W., "Carbene Chemistry", 2nd ed., Academic Press, New York, 1971.

39. Herici-Olivé, G., and Olivé, S., Angew Chem. 88, 144 (1976).

Table 1

Rate Parameters Appearing in Eqn. 1

	This Study	Vannice(5,6)	Dalla Betta et al. (1)
Catalyst	5% Ru/SiO_2	5% Ru/Al_2O_3	1.5% Ru/Al_2O_3
$A(sec^{-1}\ torr^{y-x})$	5.6×10^6	7.4×10^5	3.1×10^5
E(Kcal/mole)	24.1	24.2 $\pm$ 1.2	24
X	1.5	1.6 $\pm$ 0.1	1.8
Y	-0.6	-0.6 $\pm$ 0.1	-1.1

Table 2

Integrated Product Yields Obtained

During Reduction of Carbonaceous Residues

Steady-State Conditions				Reduction Conditions		Integrated Product Yield	
T(°C)	P_{CO}(torr)	P_{H_2}/P_{CO}	t(min)	P_{H_2}(torr)	Q_{H_2}(cm^3/min)	CH_4(μmoles)	C_2H_6(μmoles)
275	100	3	70	301	237	34.7	-
225	101	3	70	299	233	16.0	-
191	100	3	70	281	193	16.2	-
191	97	6	70	292	232	33.3	-
191	16	6	70	244	194	2.6	-
191	17	3	70	220	197	1.4	-
191	186	2	70	304	140	48.6	5.4
191	195	2	120	276	196	49.2	3.4
191	195	2	90	251	227	43.9	-
191	201	1	90	232	212	15.7	-
191	223	0	70	222	211	2.5	-

Figure Captions

Fig. 1 Reactor cross-sectional view.

Fig. 2 Effect H_2/CO ratio at fixed CO partial pressure on the rate of methane formation and catalyst deactivation.

Fig. 3 Effect of CO partial pressure at fixed H_2/CO ration on the rate of methane formation and catalyst deactivation.

Fig. 4 Comparison of calculated and experimental rates of methane synthesis.

Fig. 5 Dependence of product selectivity on temperature.

Fig. 6 Dependence of product selectivity on CO partial pressure.

Fig. 7 Dependence of product selectivity on H_2/CO ratio.

Fig. 8 Infrared Spectra taken under reaction conditions: a) background at T=275°C; b) during reaction of T=275°C, P_{CO}=99 torr, P_{H_2}/P_{CO} = 3; c) during reaction at T=225°C, P_{CO}=102 torr, P_{H_2}/P_{CO}=3; d) during reaction at T=191°C, P_{CO}=197 torr, P_{H_2}/P_{CO}=2.

Fig. 9 CO band absorbance as a function of CO partial pressure. H_2/CO ratio, and temperature.

Fig. 10 Infrared spectra showing reactivity of hydrocarbon adspecies: a) background; b) during reaction at T=191°C, P_{CO}=195 torr, and P_{H_2}/P_{CO}=2; c) following elution of H_2; d) following elution of H_2 and CO; e) 2.5 min following admission of H_2/He mixture; f) 4.5 min following admission of H_2/He mixture; g) 7.5 min following admission of H_2/He mixture.

Fig. 11 Response of CO band absorbance and CO partial pressure during catalyst reduction following steady state reaction: P_{CO} = 16 torr.

Fig. 12 Relative rates of methane and ethane production during catalyst reduction following steady state reaction: P_{CO} = 16 torr (Arrows indicate the time at which the CO band absorbance goes to zero.)

Fig. 13 Response of CO band absorbance and CO partial pressure during catalyst reduction following steady state reaction: P_{CO} = 100 torr.

Fig. 14 Relative rates of methane and ethane production during catalyst reduction following steady state reaction: P_{CO} = 100 torr. (Arrows indicate the time at which the CO band absorbance goes to zero.)

Fig. 15 Relative rates of methane and ethane production during catalyst reduction following steady state reaction: P_{CO} = 195 torr. (-●- CO eluted by H_2/He stream; -▲- CO eluted by He prior to introduction of H_2/He stream)

Fig. 16 CO adsorption isotherms (24).

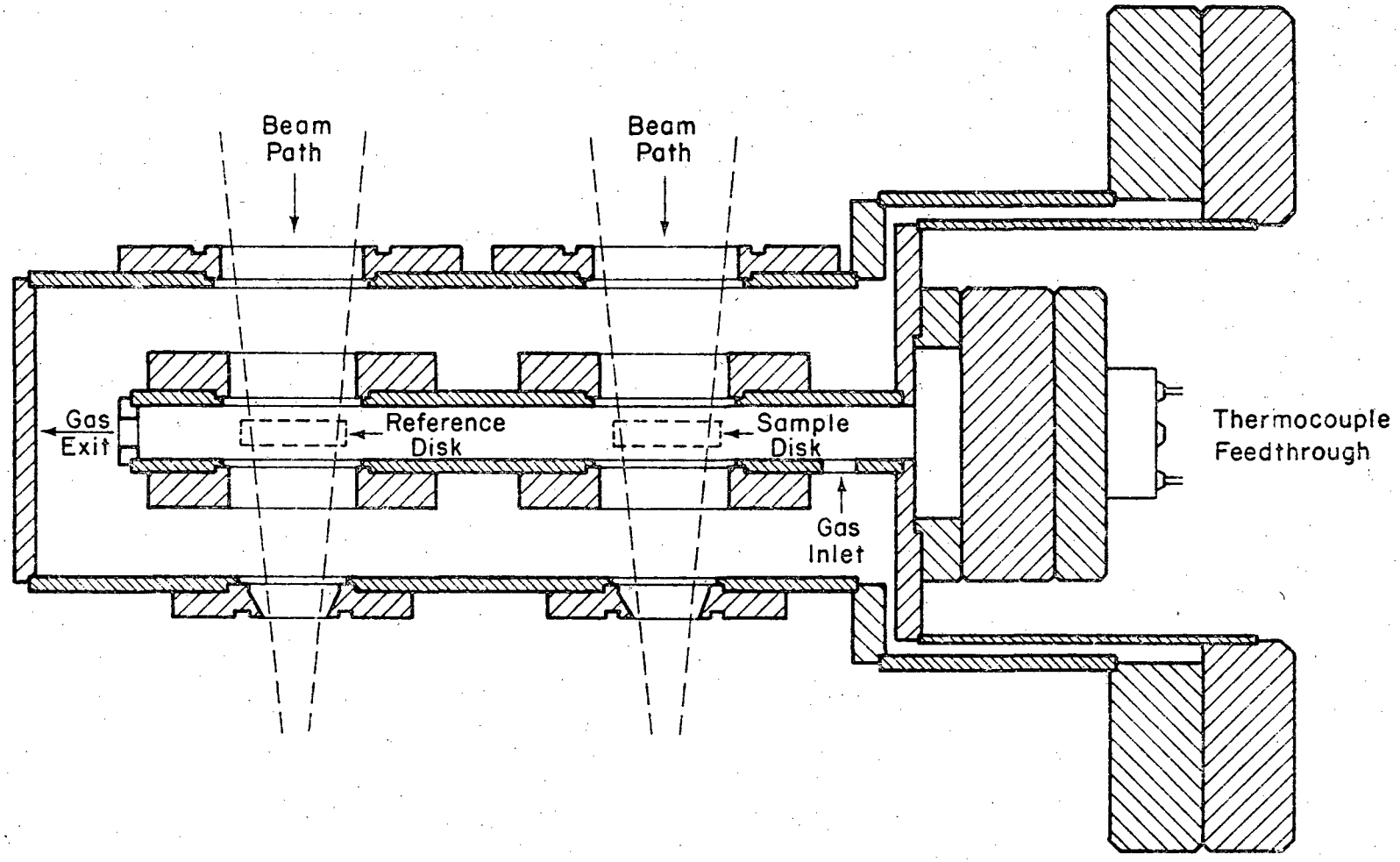

Figure 1.

XBL 784-8314

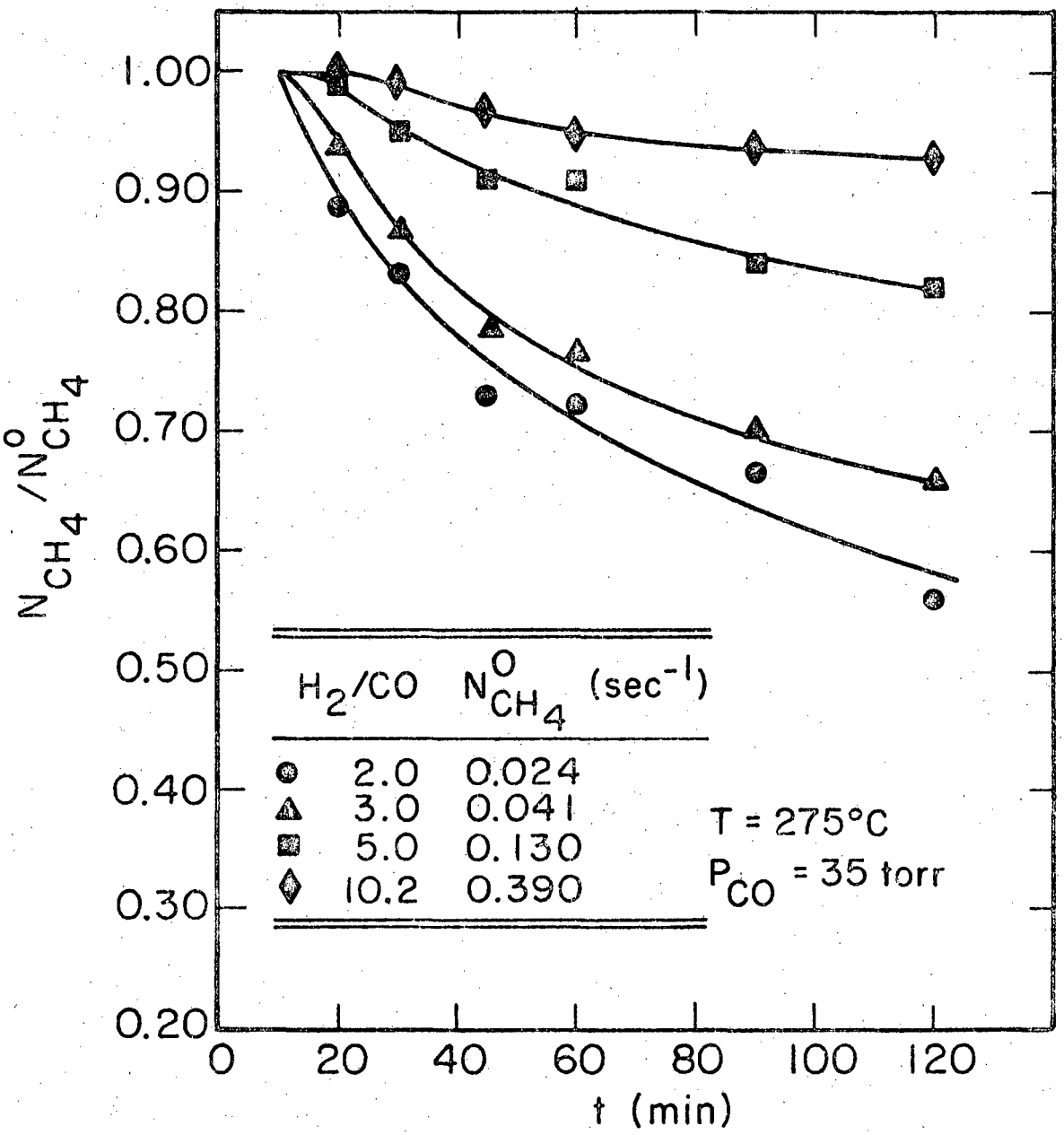

XBL 788-10062

Figure 2.

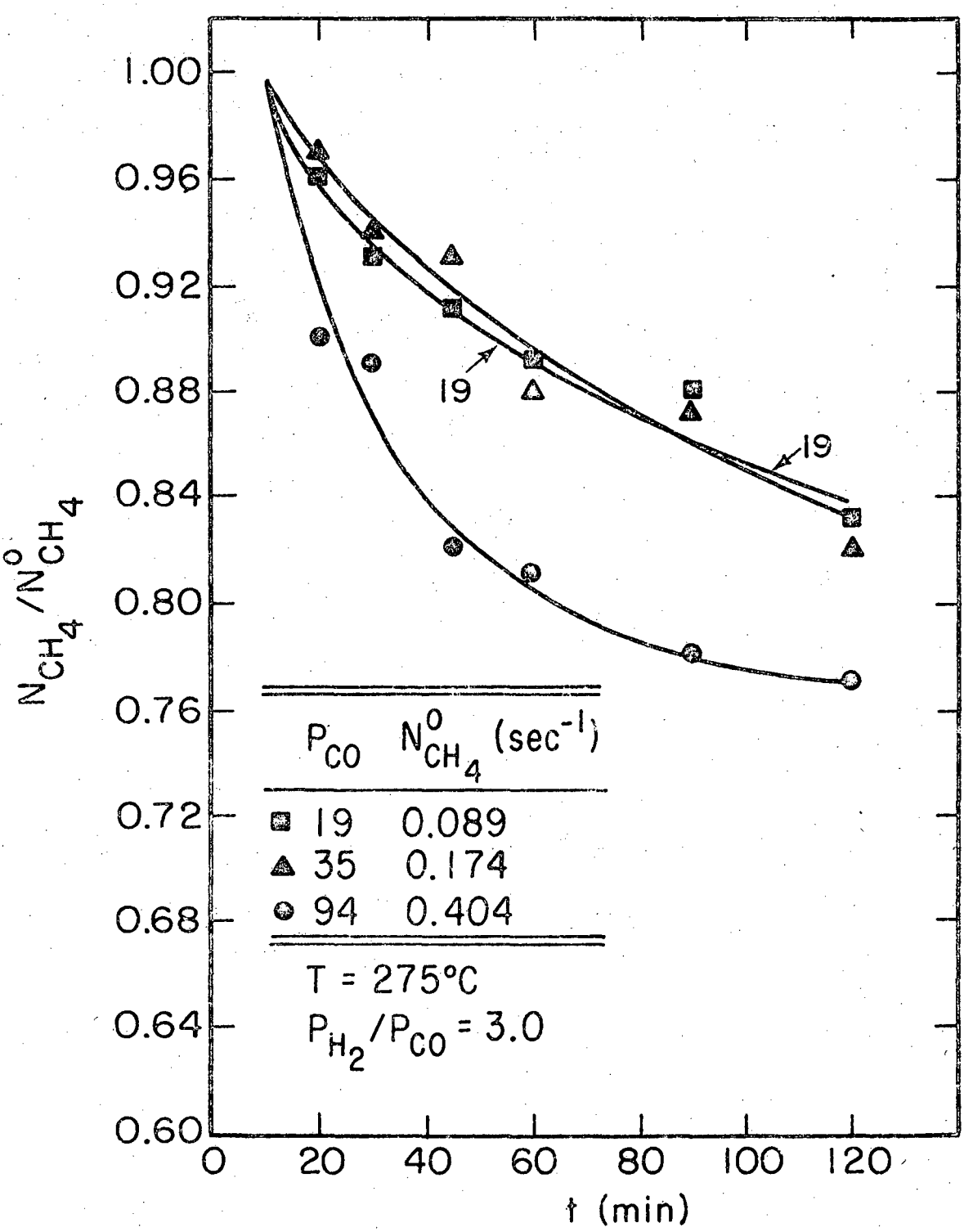

XBL 788-10059

Figure 3.

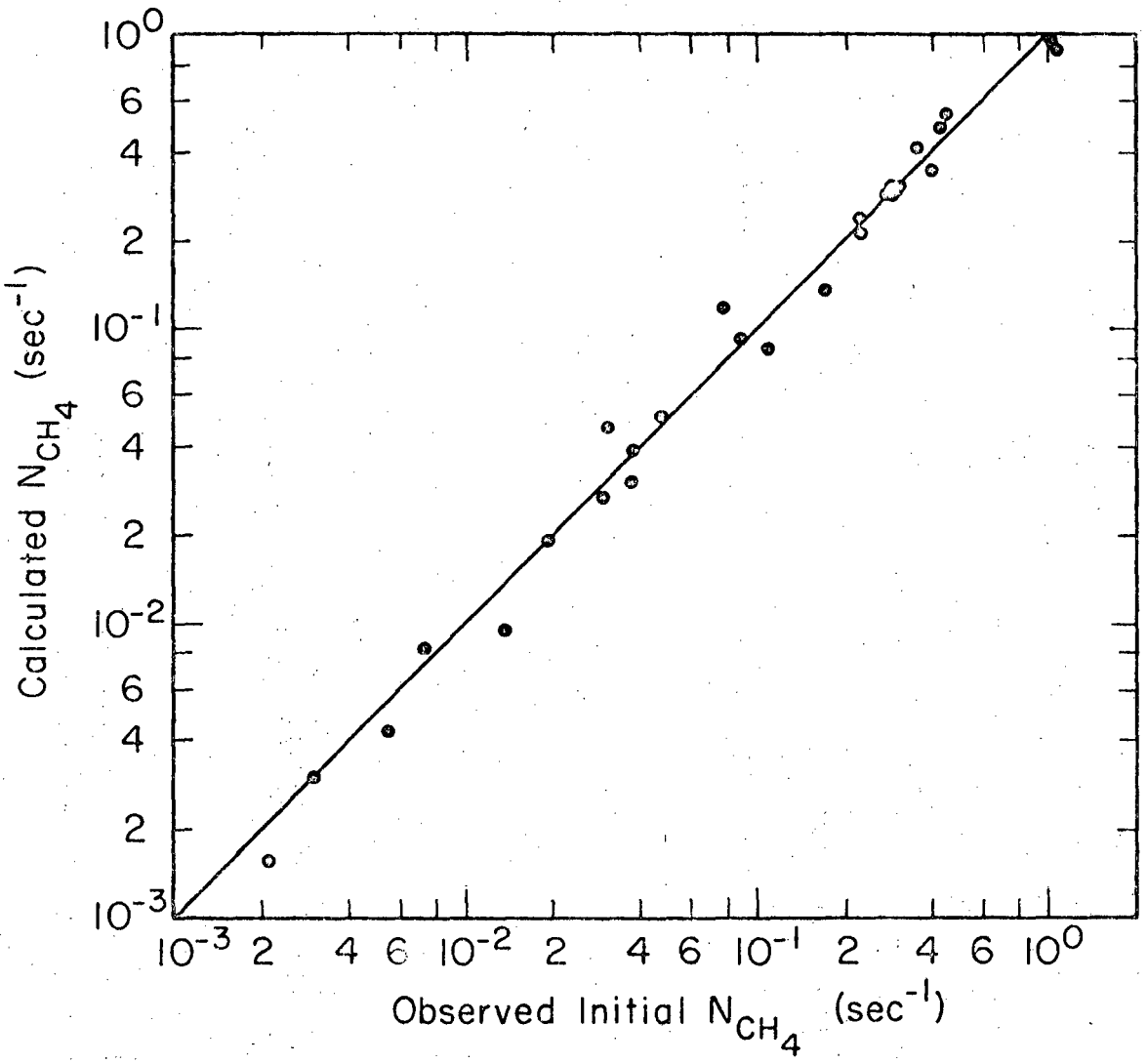

Figure 4. XBL 788-10066

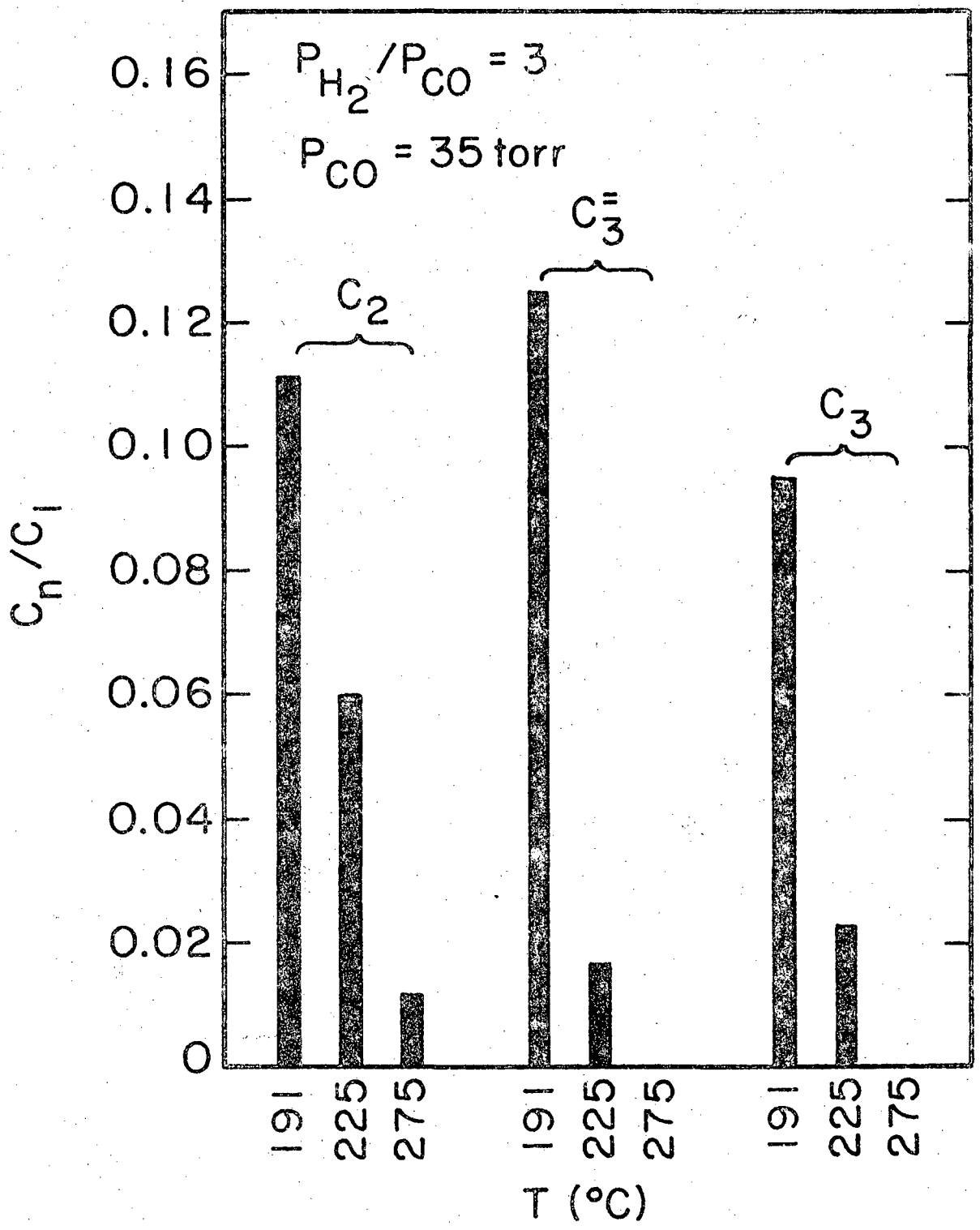

XBL 788-10061

Figure 5.

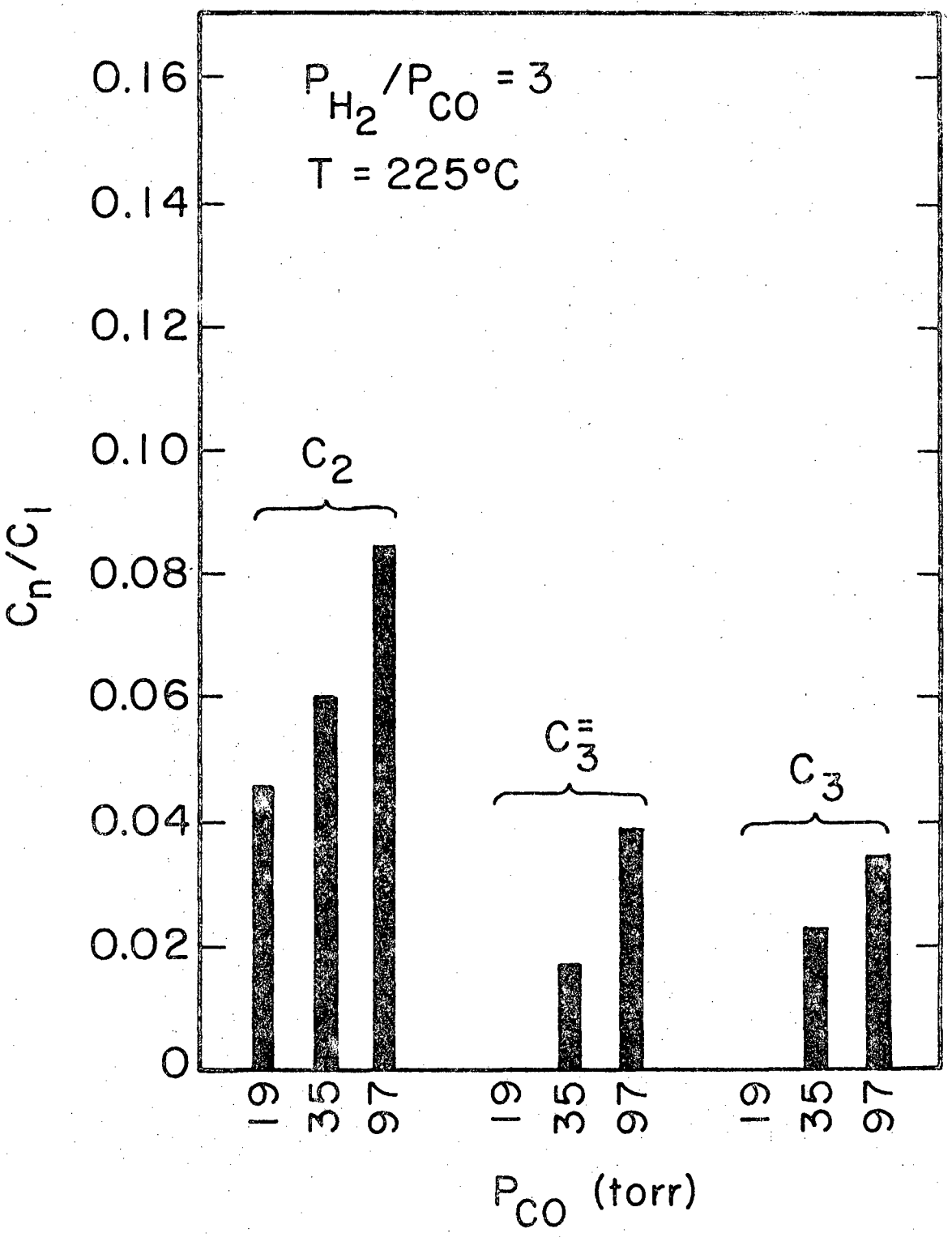

XBL 788-10060

Figure 6.

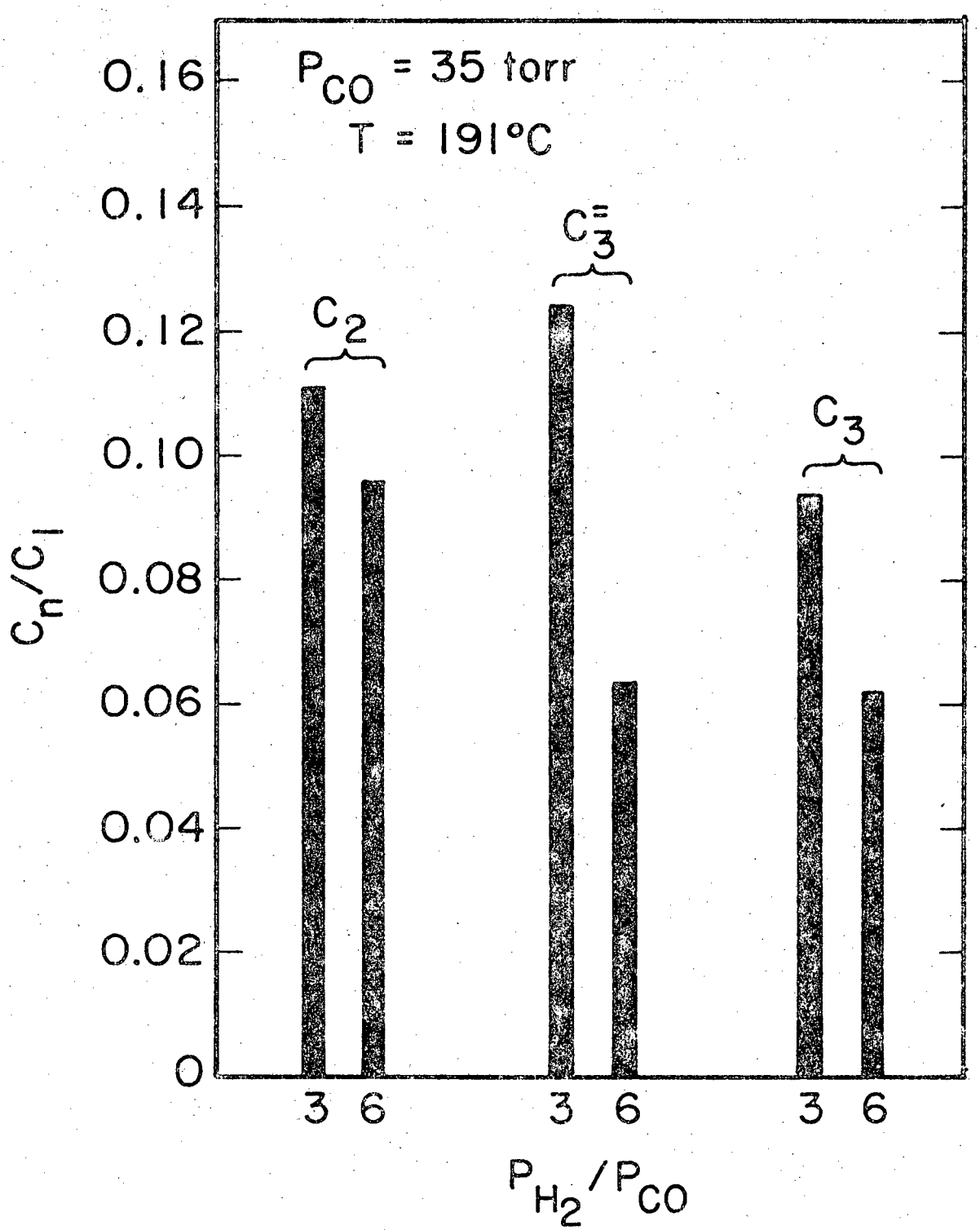

XBL 788-10058

Figure 7.

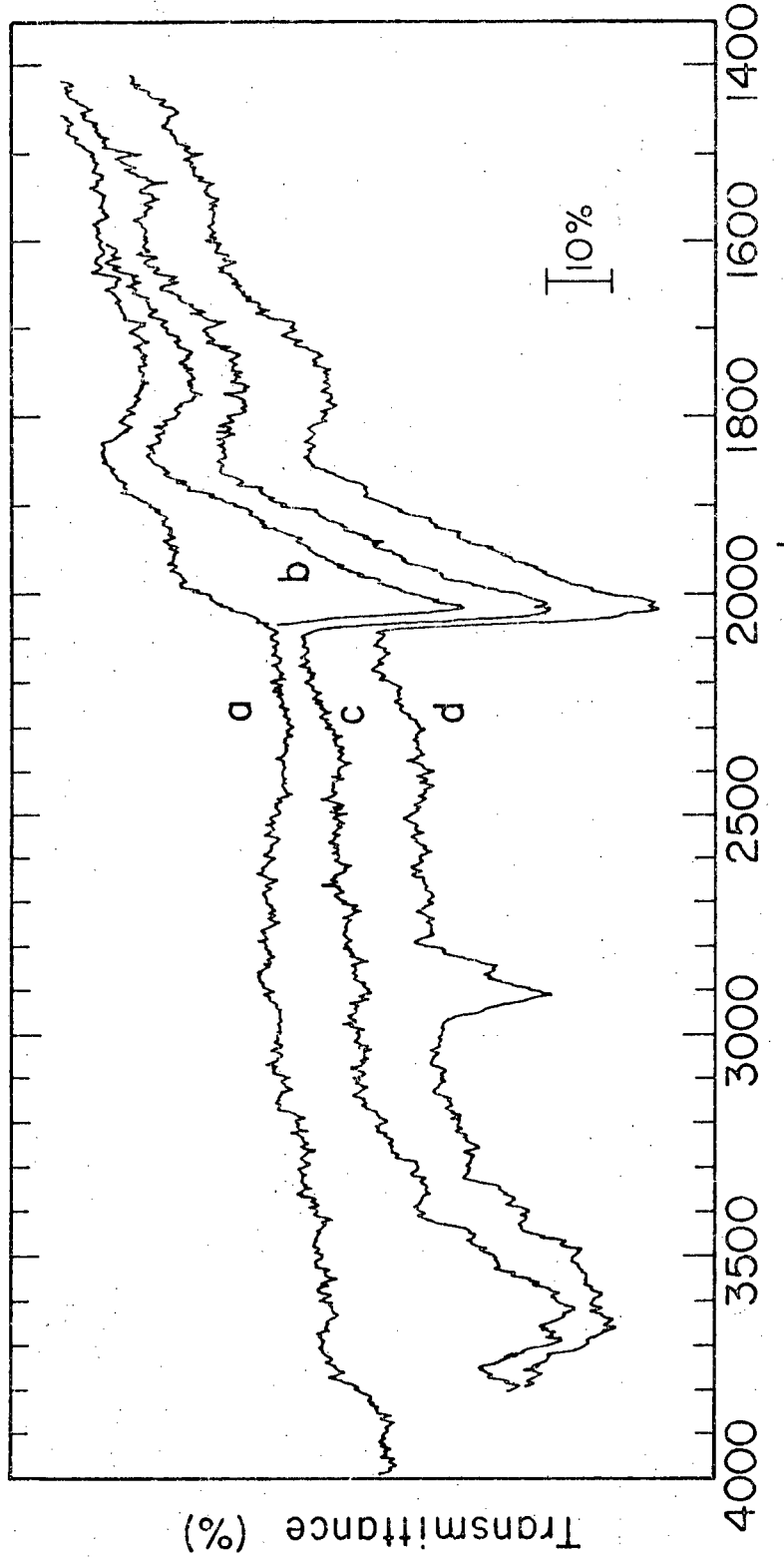

XBL 788-10070

Figure 8.

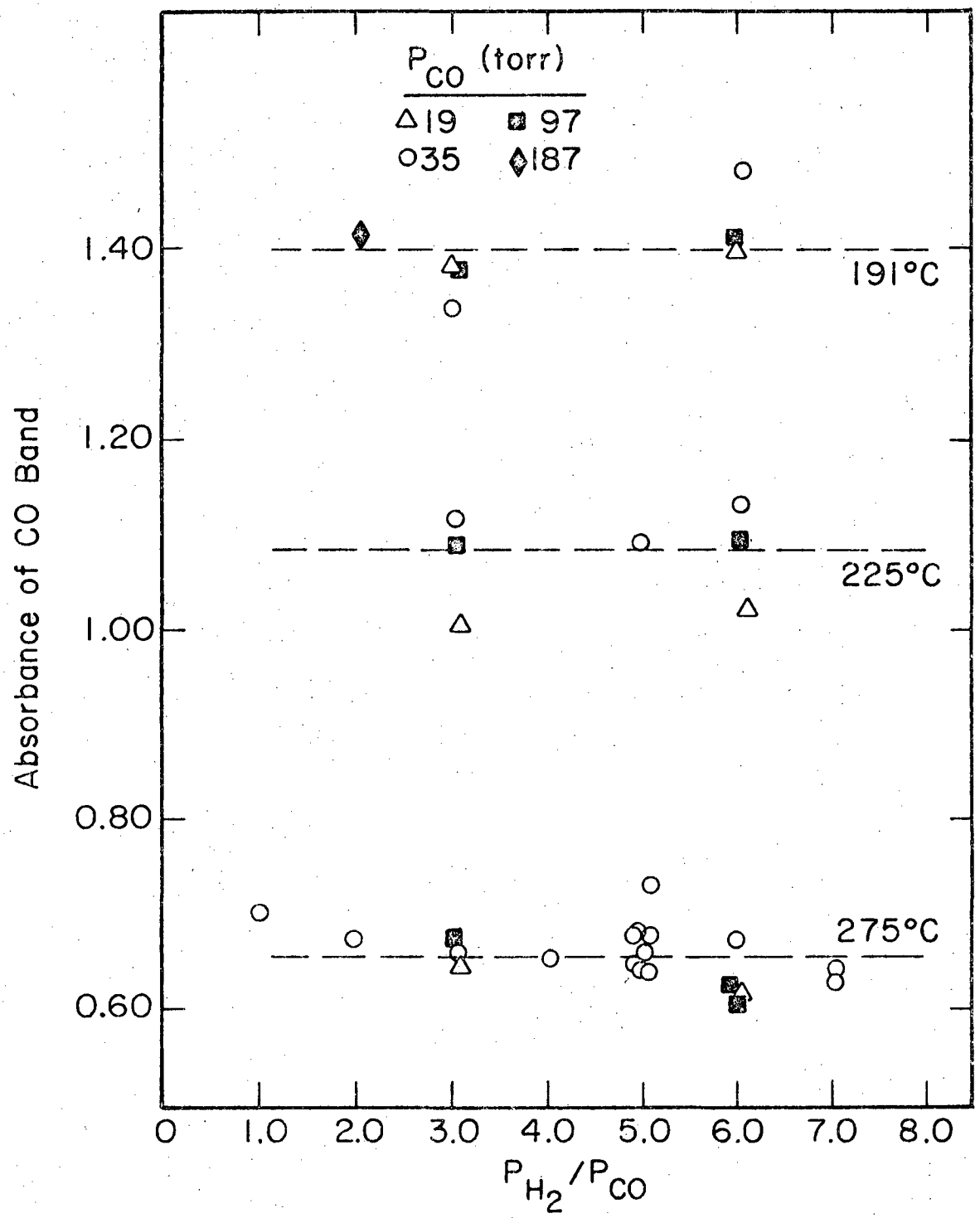

XBL 788-10065

Figure 9.

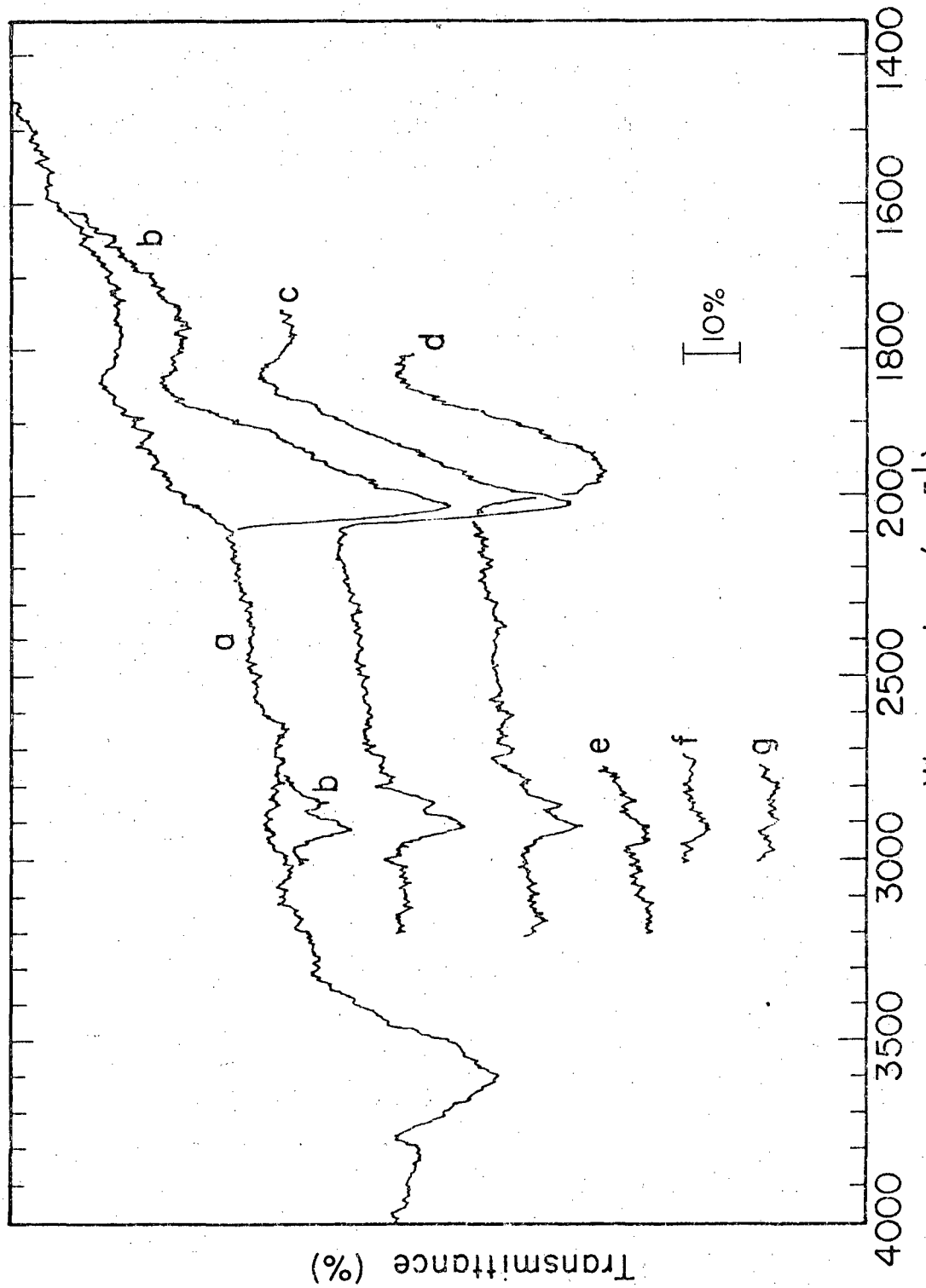

XBL 788-10059

Figure 10.

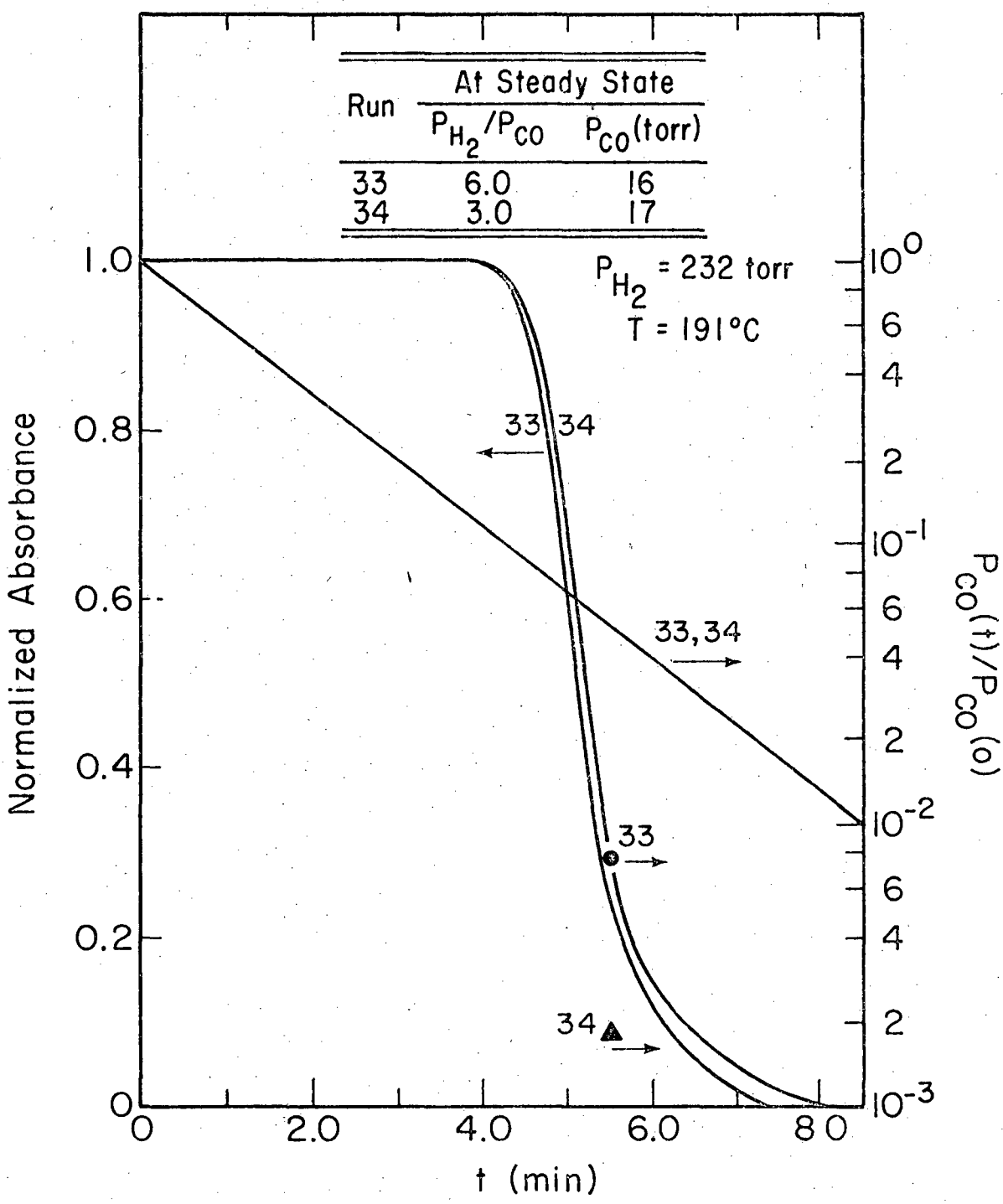

Figure 11. XBL 788-10063

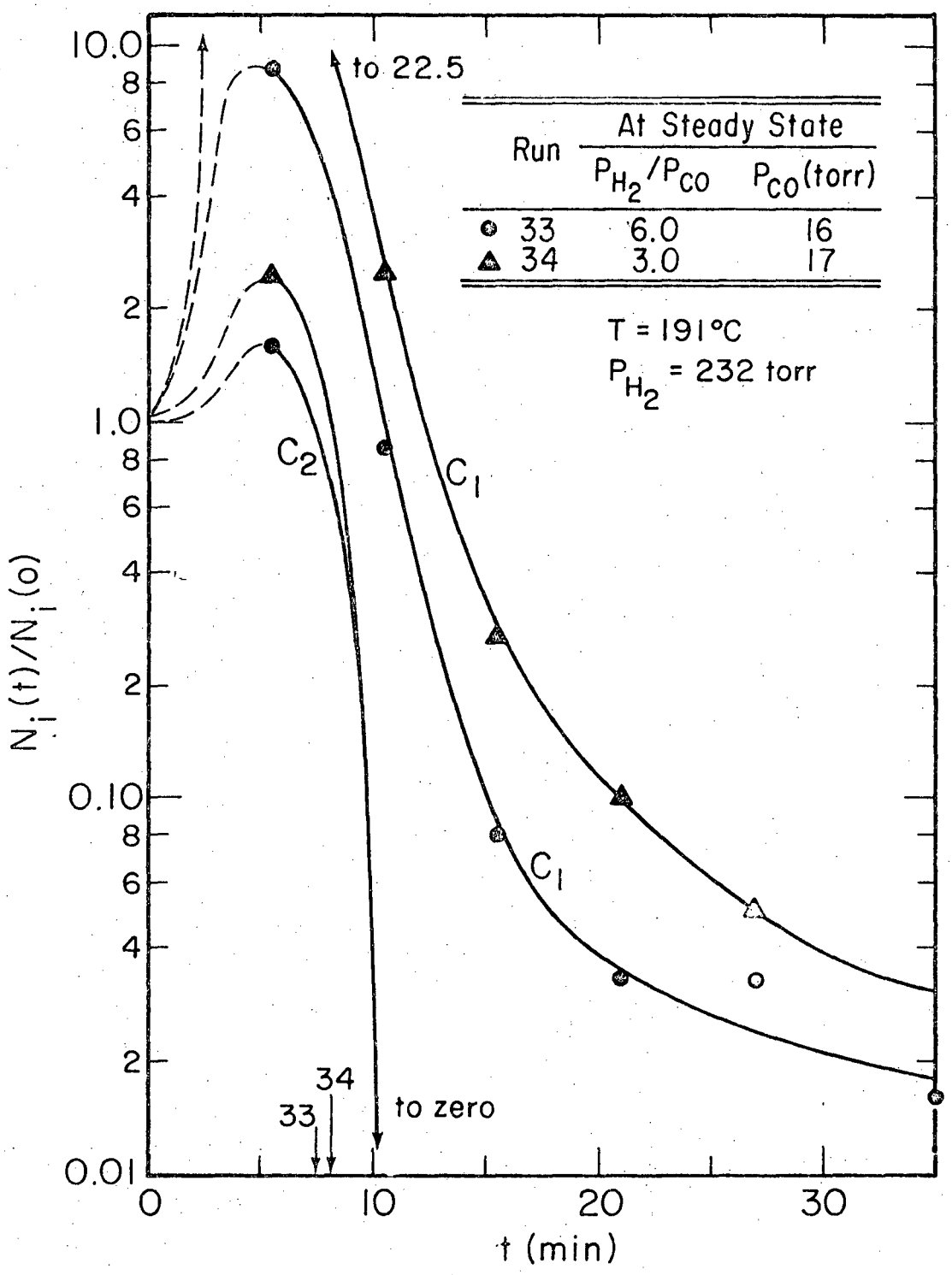

XBL 788-10064

Figure 12.

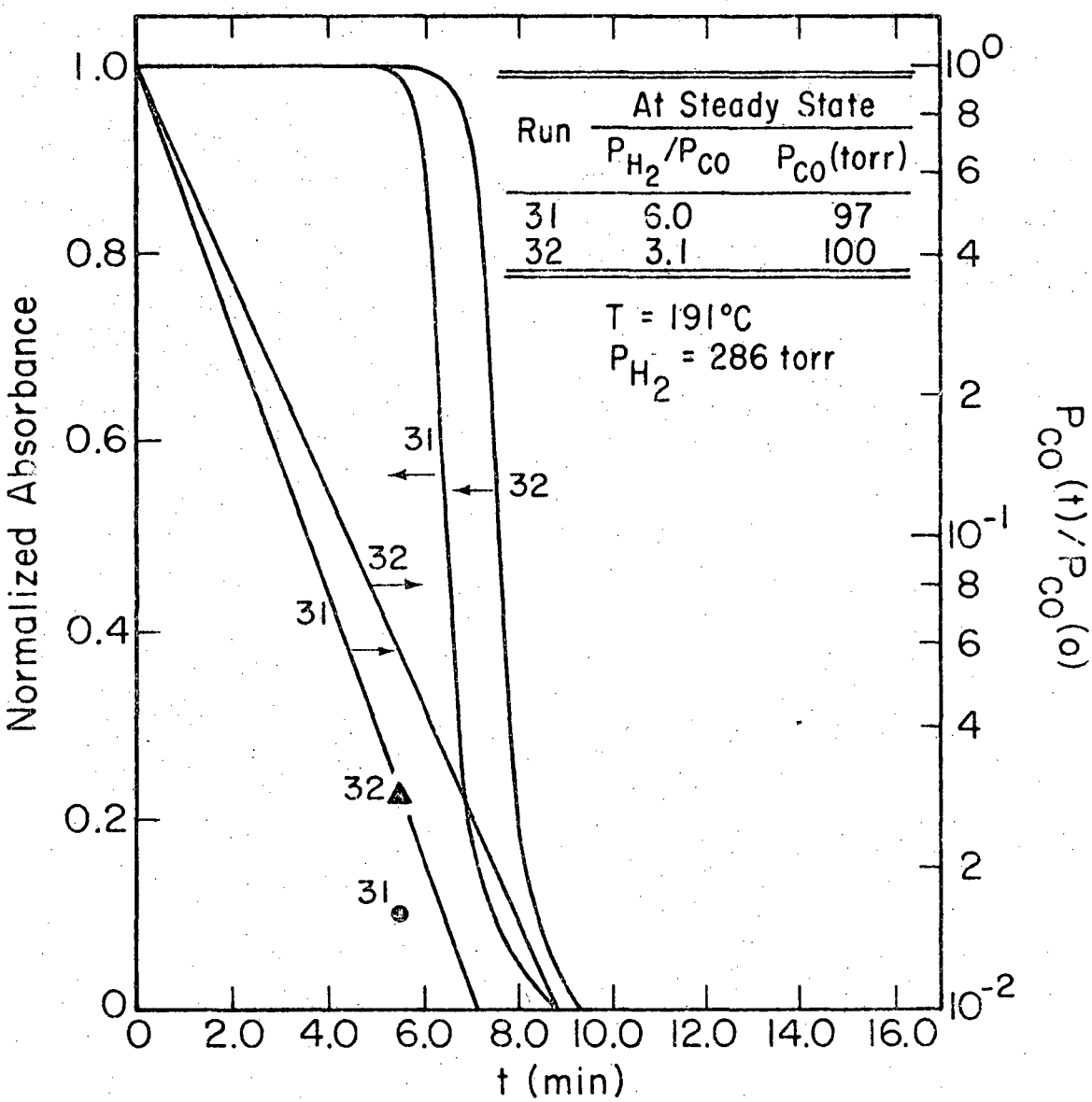
Normalized Absorbance
1.0
0.8
0.6
0.4
0.2
0
0 2.0 4.0 6.0 8.0 10.0 12.0 14.0 16.0
t (min)
$P_{CO}(t)/P_{CO}(o)$
10^0
8
6
4
2
10^{-1}
8
6
4
2
10^{-2}
Run
At Steady State
P_{H_2}/P_{CO}
P_{CO}(torr)
31 6.0 97
32 3.1 100
T = 191°C
P_{H_2} = 286 torr
31
32
32
31
32
31
XBL 788-10068

Figure 13.

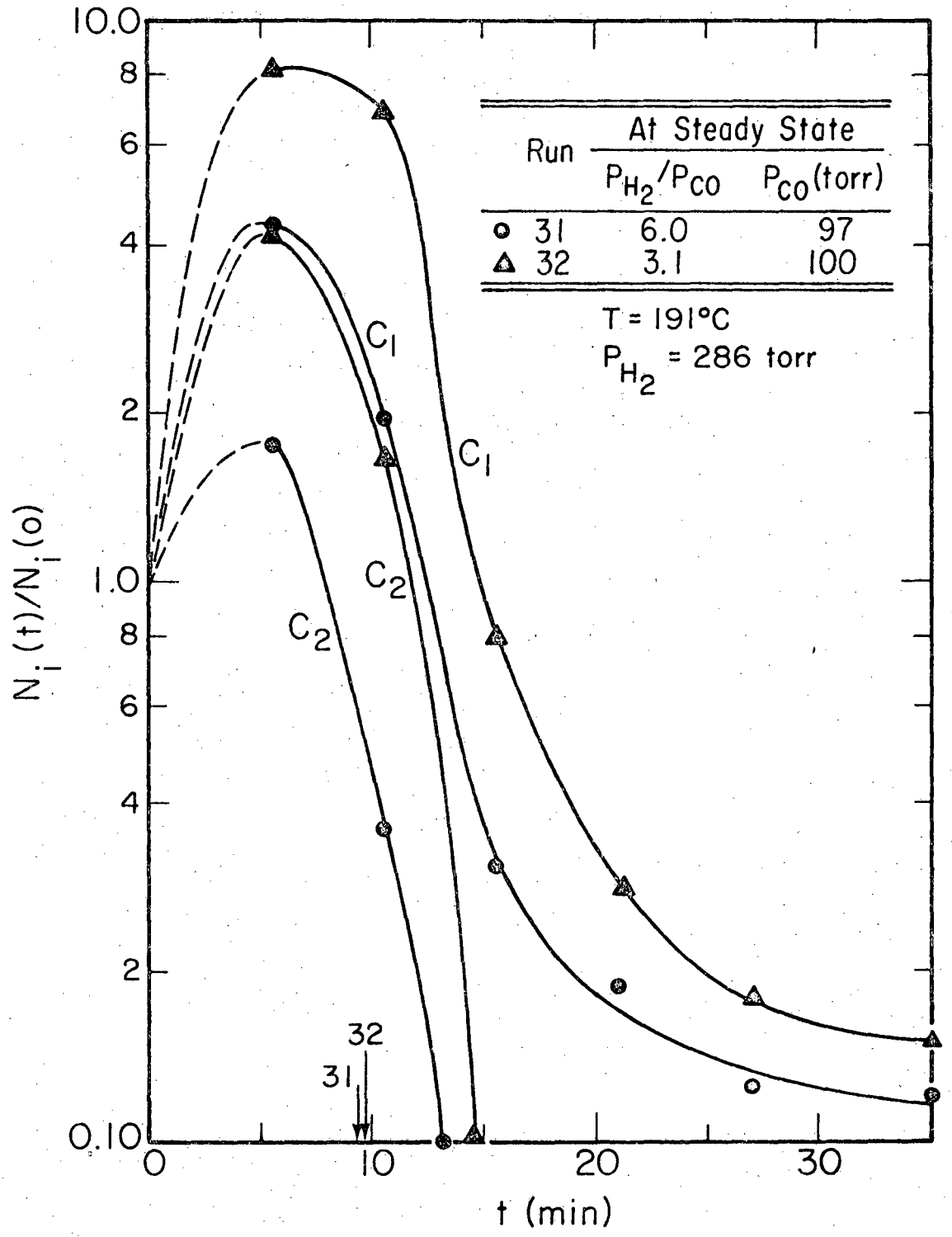

XBL 788-10067

Figure 14.

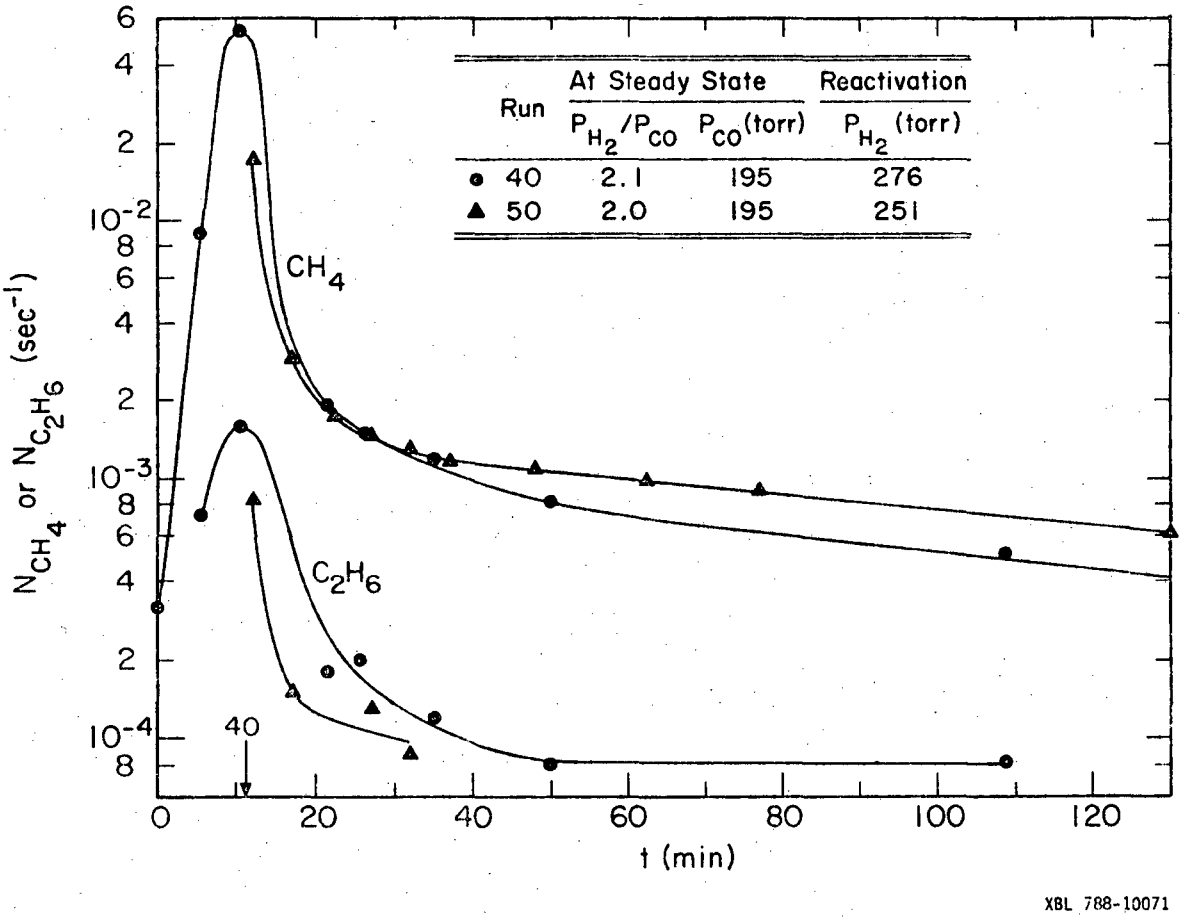
Run
At Steady State
P_{H_2}/P_{CO}
P_{CO}(torr)
Reactivation
P_{H_2} (torr)
40 2.1 195 276
50 2.0 195 251
CH_4
C_2H_6
40
N_{CH_4} or $N_{C_2H_6}$ (sec^{-1})
t (min)
XBL 788-10071

Figure 15.

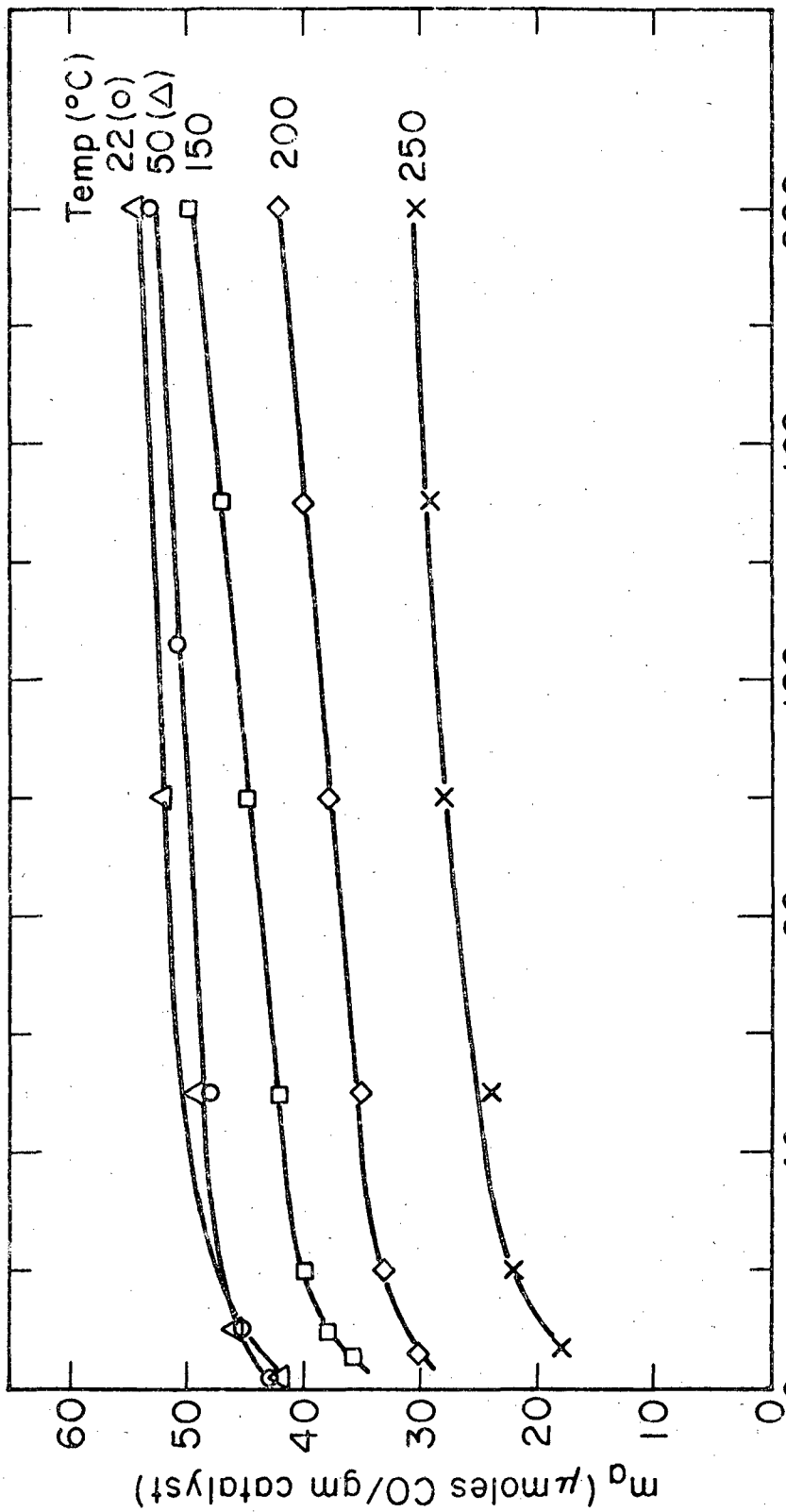

XBL765-5477

Figure 16.

This report was done with support from the Department of Energy. Any conclusions or opinions expressed in this report represent solely those of the author(s) and not necessarily those of The Regents of the University of California, the Lawrence Berkeley Laboratory or the Department of Energy.

TECHNICAL INFORMATION DEPARTMENT
LAWRENCE BERKELEY LABORATORY
UNIVERSITY OF CALIFORNIA
BERKELEY, CALIFORNIA 94720